# Response to the comments of Reviewer 2

First of all, we would like to thank the anonymous reviewer for the careful review and valuable suggestions. We carefully revised the manuscript following the suggestions. Hereby we give a point-by-point reply to address the comments. In this document, the words in *italics are the reviewers' comments*, the words in blue are the modifications we have made in the revision, and others are our responses.

**Q1:** *The manuscript Antarctic snow-covered sea ice topography derivation from TanDEM-X using polarimetric SAR interferometry by Huang et al. presents the development and validation of a new two-layer plus volume sea ice model with the aim to correct for the height bias associated with InSAR penetration into the snow pack. This model is able to represent the sea ice/snow stratigraphy and associated scattering, and, when simplified and inverted, allows for the estimation of the sea ice plus snow surface topography from TanDEM-X. This retrieval technique shows strong agreement to an Operation IceBridge optical (DMS) DEM that was collected contemporaneously as part of the OIB/TanDEM-X Coordinated Science Campaign. This manuscript is well-written and thoroughly presents novel methods and results that could be useful to the broader sea ice community. I have a few relatively minor comments and suggestions that should be considered, found in the general and specific comments below. The main comments I have on the manuscript deal with (1) the height threshold used (2) X-band scattering/slush layers and (3) the snow depth parameter.*

**A1:** We thank the reviewer for the positive comment about our research. We have carefully revised the manuscript based on the following comments.

**Q2:** *GC1: To me, it appears there is some mix-up with the height threshold used to keep model-error accuracy to within 25volume (z1-z2) needs to be thicker than 1.5m to achieve this accuracy. However, in later sections only ice+snow heights above the local sea surface (effectively the total freeboard) above 1.5m are used. Doing so filters out ice volumes much thicker than 1.5m, since most of the ice volume is below the waterline. I would suggest the authors confirm that the 1.5m threshold is indeed for the ice volume, and recommend that they filter the InSAR retrieved heights accordingly (which should result in a much lower height-above-sea-surface threshold).*

**A2:** We confirm that the $\sim 1.5\,\mathrm{m}$ threshold is for the ice volume to achieve a $\leq 25\%$-error inversion accuracy. In the revision, the applied height threshold was change to $0.8\,\mathrm{m}$ in order to select ice that is deformed and thick without seawater flooding (see Fig. 1(b)). In this case, ice thickness should exceed $2\,\mathrm{m}$ (**see details in A3**), corresponding to surface height of $\sim 0.8\,\mathrm{m}$ (Ozsoy-Cicek et al., 2013). Therefore, the samples with height above $0.8\,\mathrm{m}$ are selected for processing. In the revision, experimental parts have been updated as suggested, and the sentences below have been added in the new Section 2.1:

"The relation between ice thickness $H_i$ and surface height $h_{\mathrm{sur}}$ (i.e., ice height above sea surface including snow depth) has been discussed over different regions (Petty et al., 2016; Toyota et al., 2011; Ozsoy-Cicek et al., 2013). Ozsoy-Cicek et al., (2013) showed a linear relation $H_i = c_0 h_{\mathrm{sur}} + c_1$ with $c_0 = 2.24$ and $c_1 = 0.228$ fitted from large-scale, survey-averaged data over the Western Weddell Sea, which is the same region as this study. According to this linear relation, $H_i = 2\mathrm{m}$ corresponds to a surface height of $\sim 0.8\,\mathrm{m}$."

**Q3:** *GC2: (This is similar to that from reviewer 1) While the scattering impacts of a slush layer are briefly mentioned, I feel that their impact should either be discussed further or/and incorporated into the model in some way. A slush layer at* *the snow-ice interface would surely effect the radar return differently than if the snow-ice interface was smooth and dry. Also, some mention of the effects of surface roughness would be beneficial, as snow surface/interface roughness has been found to influence X-band backscatter (Nandan et al. 2016, Remote Sens. Of Envir., https://doi.org/10.1016/j.rse.2016.10.004). Finally, while surface melt may not be present in this particular region or season, a wet snow surface could also influence the X-band backscatter (Dufour-Beauséjour et al. 2020, The Cryosphere, https://doi.org/10.5194/tc-14-1595-2020). This would need to be taken into account if applying this technique to other regions and/or seasons.*

**A3:** We agree that the slush layer is important for Antarctic sea ice. In the revision, we have added more references introducing the slush layer in Section 1 (Introduction):

"In the Arctic first-year thin ice, snow capillary force gives rise to brine wicking, and consequently, a layer of high salinity slush ice appears at the snow-ice interface (Reimnitz and Kempema, 1987; Drinkwater and Crocker, 1988; Nghiem et al., 1995a). In the Antarctic, ice-surface flooding widely occurs resulting from the generally thicker snow layer loading on the thinner ice floes, often followed by freezing of the slush layer at the snow-ice interface (Massom et al., 2001; Jeffrieset al., 2001; Maksym and Jeffries, 2000). Even without flooding, the upward wicking of brine from the ice surface can also form a saline layer at the bottom of the snowpack (Massom et al., 2001; Toyota et al., 2011; Webster et al., 2018). The slush layer at the snow-ice interface would induce significant surface scattering and thus has been included in the sea ice scattering modelling (Nghiem et al., 1995a, b; Maksym and Jeffries, 2000)."

Besides, focusing on the Antarctic sea ice, we have added more explanations about the slush layer for both thinner and thicker ice conditions in Section 2 (Basic concepts). Different sea ice structures for thinner ice and thicker ice have been plotted in Fig. 1(a) and (b), respectively. We have also emphasized that in this study, the experiments are conducted based on the thicker and deformed ice with height $> 0.8\,\mathrm{m}$ above the sea level. This height threshold is estimated from hydrostatic balance, and we assume that sea ice higher than this threshold do not suffer seawater flooding. Note that even without flooding, the upward wicking of brine from the ice surface can also form a thin and high saline layer at snow-ice interface (Massom et al., 2001; Toyota et al., 2011; Webster et al., 2018). Therefore, the surface scattering from the slush layer at the snow-ice interface has been considered in the model. Below Fig. 1 and texts have been added in the new Section 2.1:

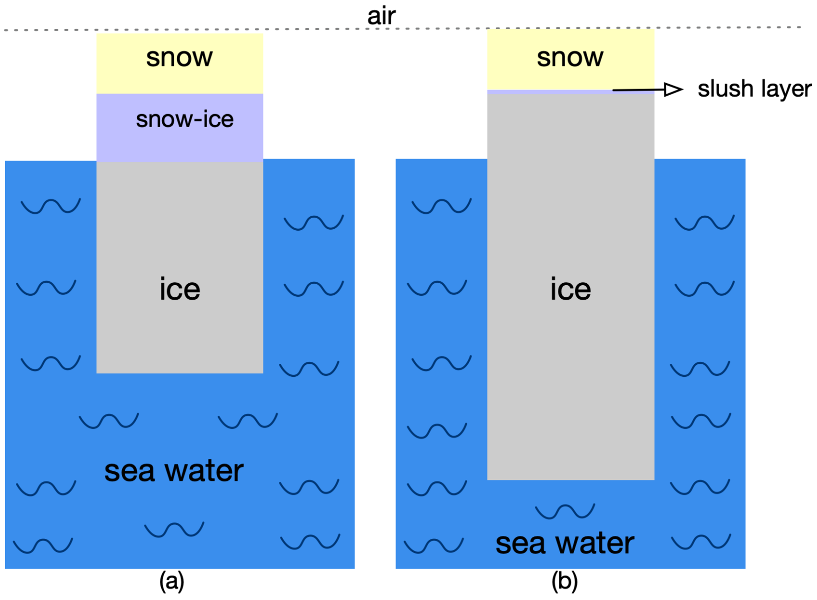

Fig. 1: Schematic of (a) thinner ice floes flooded by seawater and (b) thicker ice floes without flooding.

"In the Antarctic, the presence of a saline layer at the snow-ice interface due to the flooding or capillary suction of brine from the ice surface has been recognized as a widespread and critical phenomenon (Massom et al., 2001). For thinner ice, flooding may occur when the weight of the snow pushes the ice surface below the water level, yielding a negative freeboard. In this case, as shown in Fig. 1(a), seawater infiltrates into the snowpack, floods the ice surface, and creates a high-saline slush layer which may refreeze into snow ice (Lange et al., 1990; Jeffries et al., 1997; Maksym and Jeffries, 2000). The thickness of snow ice was observed to be $\sim 42-70\%$ of the total snow accumulation (i.e., the thickness of snow ice plus snow depth) (Jeffries et al., 2001).

For thicker and deformed ice with ridges, less flooding occurs due to the increased buoyancy of the ice mass contained in the ridges (Jeffries et al., 1998). However, even in the absence of flooding, a thin slush layer can also occur due to the capillary suction of brine from the ice surface (Massom et al., 2001; Webster et al., 2018). Besides, the deformed ice in the ridging and rafting area is often poorly consolidated, and thus seawater may reach the snow layer and form a thin slush layer (Maksymand Jeffries, 2000). The sea ice structure for thicker ice without flooding is sketched in Fig. 1(b), including snow on top, the ice volume, and a thin and high-saline layer in between.

The condition of flooding can be quantified by a simple hydrostatic balance (Lange et al., 1990)

$$\begin{aligned} \rho_w d &= \rho_i d + \rho_i f + \rho_s s \\ t &= d + f \end{aligned} \tag{1}$$

where $\rho_w$, $\rho_i$, and $\rho_s$ are the densities of seawater, ice, and snow, respectively; $d$, $f$, $t$ and $s$ are the thickness of ice below and above the sea level, the total ice thickness, and the snow depth on top, respectively. For flooding to occur, $f$ should be zero (i.e., $d = t$), and Eq. (1) becomes

$$s/t = (\rho_w - \rho_i)/\rho_s \approx 0.12/\rho_s \tag{2}$$

by assuming $\rho_w = 1.03\,\mathrm{Mg/m^{-3}}$ and $\rho_i = 0.91\,\mathrm{Mg/m^{-3}}$ (Lange et al., 1990). For snow density $\rho_s$ being $0.3\,\mathrm{Mg/m^{-3}}$ (Lange et al., 1990), the ratio between snow depth and ice thickness $s/t$ is estimated to be $0.4$. The snow depth on Antarctic sea ice during September and November was shown to be below $0.8\,\mathrm{m}$ for $99\%$ of the samples in Webster et al., (2018). This range of snow depth will lead to flooding for ice thickness $< 2\,\mathrm{m}$.

The relation between ice thickness $H_i$ and surface height $h_{\mathrm{sur}}$ (i.e., ice height above sea surface including snow depth) has been discussed over different regions (Petty et al., 2016; Toyota et al., 2011; Ozsoy-Cicek et al., 2013). Ozsoy-Cicek et al., (2013) showed a linear relation $H_i = c_0 h_{\mathrm{sur}} + c_1$ with $c_0 = 2.24$ and $c_1 = 0.228$ fitted from large-scale, survey-averaged data over the Western Weddell Sea, which is the same region as this study. According to this linear relation, $H_i = 2\mathrm{m}$ corresponds to a surface height of $\sim 0.8\,\mathrm{m}$.

This paper focuses on thicker ($> 2\,\mathrm{m}$) and deformed ice (Fig. 1(b)), which is the main ice typology in the studied area. In the following sections, the model and experiments are conducted only for the samples above $\sim 0.8\,\mathrm{m}$ surface height. We assume that samples exceeding this threshold are thicker and deformed ice without flooding. The potential to extend the proposed model to thinner ice scenarios (e.g. Fig. 1 (a)) is discussed in Section 7.3."

The Figure: Schematic of the proposed two-layer plus volume model for sea ice, has been updated with Fig. 2 and some sentences have been added in Section 4.2:

"The top layer located at $z_1$ is the snow-ice interface, which can induce significant surface scattering due to a slush layer

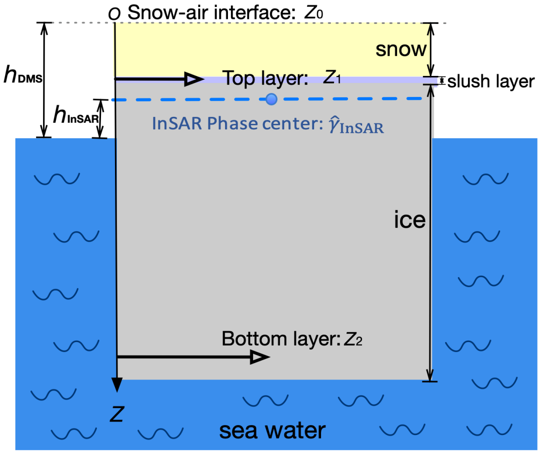

Fig. 2: Schematic of the proposed two-layer plus volume model for the thicker and deformed sea ice.

with high permittivity (Hallikainen and Winebrenner, 1992; Maksym and Jeffries, 2000). This slush layer is widespread on the Antarctic sea ice, and increases the radar backscattering as well as limits the signal penetration compared to a smooth and dry snow-ice interface. As long as the slush layer has a small vertical extent, it is irrelevant for the Pol-InSAR scattering structure model, whether the top layer represents the snow-ice interface, the snow-slush interface or both."

To extend the proposed model for thinner ice where flooding often occurs, an additional layer, i.e., snow ice formed from the slush layer when air is cold, has been discussed. A three-volume model incorporated with the snow ice could be a promising approach to correct the InSAR phase, and it will be investigated in future study. Below texts has been added in the new discussion Section 7.3:

"The proposed model was proven to be effective in a specific area covered by thick and deformed ice with snow cover in the Western Weddell Sea. The extension of the proposed model to other ice types under different environmental conditions needs further research and suitable data.

In order to apply the model over younger and thinner sea ice, the first challenge is the severe misregistration between SAR images and reference measurements due to the stronger dynamics of thinner sea ice. Reduced SAR backscattering intensity corresponding to thinner and smoother sea ice further complicates the data co-registration. Besides, the achievable height sensitivity for thin ice is also a major limitation of InSAR/Pol-InSAR derived sea ice DEMs with current SAR systems. In this study, the proposed method can achieve sea ice topographic retrieval with an $RMSE$ of $0.26\,\mathrm{m}$ for thick and deformed ice; however, this accuracy is insufficient for thinner ice whose height above sea level is only tens-of-centimeters or even less. Last but not least, an additional volume, i.e., snow ice formed by flooding, should be considered when extending the proposed model to a thinner ice area. Past studies showed that snow ice contributes an average of $8\%$ of the total volume in the Weddell Sea (Lange et al., 1990). A greater amount of snow ice, which accounts for $12-36\%$ of the total mass, was reported in the Ross, Amundsen, and Bellingshausen Seas (Jeffries et al., 2001). Although the snow ice has a higher salinity than the ice below, there could be still some penetration into the ice volume below. Therefore, in order to correct the InSAR phase center and retrieve surface height for snow-covered thin ice in the Antarctic (as illustrated in Fig. 1 (a)), a three-volume model, including snow, snow ice, and ice, would be worthy of further investigations."

Roughness plays an important role for the backscattering from surfaces and interfaces. Nandan et al., (2016) demonstrated the roughness effects through modelling, where they assume the same roughness for the snow-air surface, the snow-snow interfaces, and the snow-ice interface, for a brine-wetted snow cover on smooth FYI ice. While the scope of our Pol-InSAR model is less detailed than their ground-based study, we account for roughness induced surface/interface backscatter effects, in relative terms, by the layer-to-volume ratios and respectively the layer-to-layer ratios. However, in contrast, we neglect an air-snow surface scattering contribution due to the required simplifications for the satellite based Pol-InSAR application. Given the quite different sea ice scenario in our study, we consider this appropriate. The following explanation has been added in Section 4.2:

"An additional parameter, the layer-to-volume scattering ratio, accounts for the (relative) scattering from these interfaces, depending e.g. on roughness and dielectric contrast (Fischer et al., 2018)."

Some mentions and references describing the effects from snow surface, especially a wet snow surface effects during melting season has been added in the new discussion Section 7.3:

"To apply the model to other seasons, the snow-air surface may also be incorporated into the model since snow roughness has been found to influence X-band SAR backscatter (Nandan et al., 2016), especially for wet snow surface which often occurs during melting season (Dufour-Beauséjour et al., 2020)."

**Q4:** *GC3: The paper states that the influence of snow depth on $\gamma_{mod_T}$ is not negligible, and that a priori data from external sources must be used in the simplified model. If I understand correctly, the passive-microwave-derived snow depth data used as the sole model parameter results in a single snow depth value (18 cm) for each pixel across the scene. While I understand that high-resolution snow depth data is generally not available, this single value is likely not representative of the actual spatial snow depth distribution (and perhaps not realistic for heights ¿1.5m, as a quick hydrostatic calculation of ice thickness with this snow depth yields abnormally thick ice). Therefore, I'm curious as to the impact of the snow depth parameter on the experimental results (beyond what is shown in the simulated results of figure 8), and if/how the retrieved heights would agree with the DMS DEM under e.g. spatially-varying snow depths.*

**A4:** In this study, snow depth is assumed as a constant value across the scene due to the limited spatial resolution of available snow measurements. We agree with the reviewer that this single value is likely not representative of the actual spatial snow depth distribution. Therefore, in the revision, we have performed the whole inversion scheme and retrieved heights with various inputs of $z_1$. According to the snow depth on Antarctic sea ice reported in Webster et al., (2018), various $z_1$ are selected from $-0.05\,\mathrm{m}$ to $-0.75\,\mathrm{m}$. Using varying snow depths, we have demonstrated how the retrieved height would agree with the DMS DEM and discussed the impact of the snow depth parameter on the experimental results. Below texts and figures have been added in the revision:

"In Section 4.3, we demonstrated that the influence of snow depth on the simulated coherences is not negligible, and have stated that external data of snow measurements should be used in the model. In this study, snow depth is assumed to be invariant across the scene due to the limited spatial resolution of available snow measurements. Therefore, a constant value of $z_1 = -0.18$ is used in the retrieval. Actually, snow on sea ice undergoes temporal- and spatial-variant processes and is strongly coupled with atmospheric, oceanic, and ice conditions. Thus, a single value is not representative of the actual spatial snow depth distribution. In order to assess the impact of the snow depth on the experimental results, we perform the whole inversion scheme with various inputs of $z_1$. During September and November, the snow depth on Antarctic sea ice is reported to be maximum $\sim 1\,\mathrm{m}$ and mainly between $0$ and $0.8\,\mathrm{m}$ (Webster et al., 2018). Therefore, $z_1$ values ranging from $-0.05\,\mathrm{m}$ to $-0.75\,\mathrm{m}$ are selected. For each pixel, we retrieve heights using this range of $z_1$ values, shown as the yellow area in Fig. 3. $\Delta h_{\mathrm{mod\_S}}$ is defined as the difference between the maximum and the minimum retrieved height of every pixel. The distribution of $\Delta h_{\mathrm{mod\_S}}$ along the transect is presented in Fig. 4, where $\Delta h_{\mathrm{mod\_S}}$ has a range of $0.07 - 1.09\,\mathrm{m}$ with an average of $0.31\,\mathrm{m}$, indicating the fluctuation of model-retrieved height by using different snow depths. This analysis with various snow depth assumptions can help to constrain possible model-retrieved topographies, and $\Delta h_{\text{mod\_S}}$ can be a quantitative indicator for the uncertainty of the retrieved height in the absence of high-resolution snow depth data."

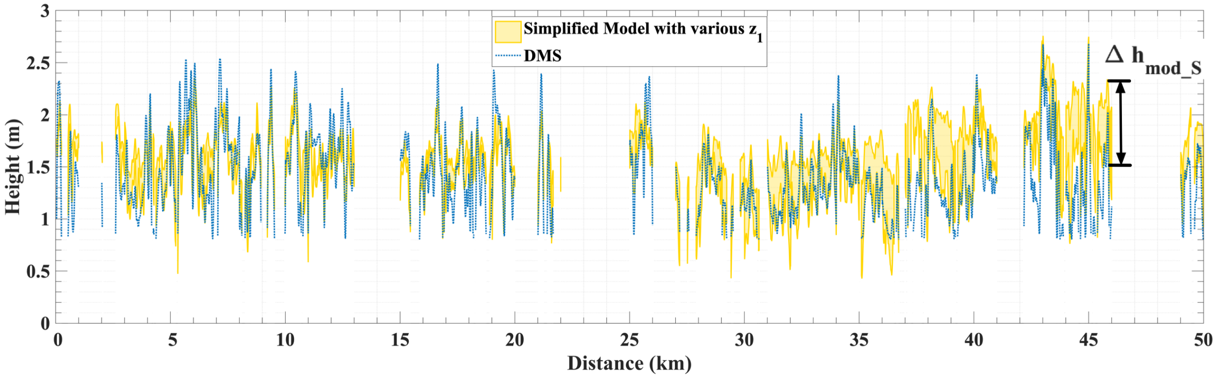

Fig. 3: Yellow area: sea ice height profiles from the simplified model in Pauli-1 polarization with $z_1$ from $-0.05\,\mathrm{m}$ to $-0.75\,\mathrm{m}$. Blue dash line: sea ice height profiles from DMS measurement. The mis-coregistered and $h_{\text{DMS}}$ below $0.8\,\mathrm{m}$ samples are excluded from the plot.

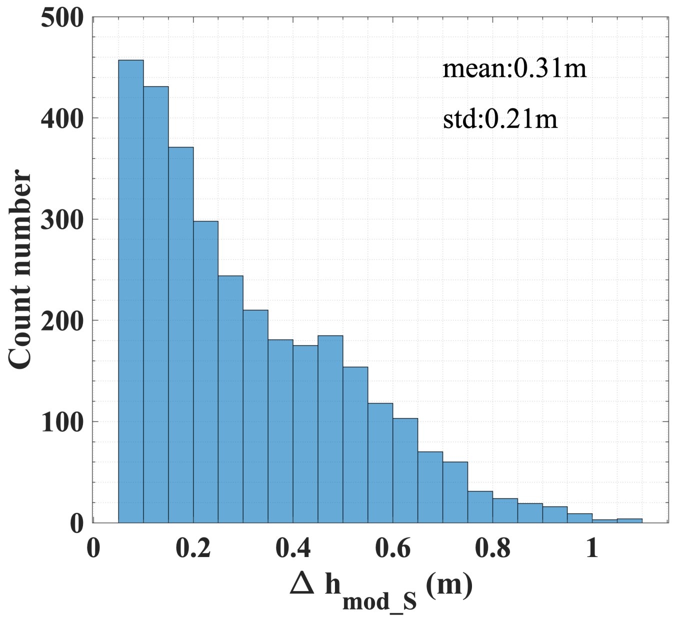

Fig. 4: The distribution of $\Delta h_{\text{mod\_S}}$ along the transect.

**Q5:** *Lines 23-25: I find this sentence slightly confusing as it's written, especially since Petty et al. 2016 also mention the "close correspondence" between the predicted (surface height+square root relation) and OIB-measured thickness. Just noting the +/-2m difference makes it sound like a poor retrieval.*

**A5:** $\pm 2\,\mathrm{m}$ is the maximum differences between measured and predicted ice thickness. Considering that the thickness in the study area varies from $0$ to $8\,\mathrm{m}$ and the IceBridge measurements of ice thickness readily include an inherent uncertainty of $0.8\,\mathrm{m}$, this study (Petty et al. 2016) provided a useful method of understanding ice topography and thickness variability. The sentences have been changed in the revision:

"Petty et al. (2016) presented a detailed characterization of Arctic sea ice topography across both first-year and multi-year sea ice and analyzed the topographic differences between the two ice regimes. A square-root relation function between sea ice topographic height and thickness was established for ice thickness retrieval (Petty et al., 2016). The results demonstrated a maximum $\pm 2\,\mathrm{m}$ difference between the measured and predicted ice thickness. Note that the measured thickness ranges from $0$ to $8\,\mathrm{m}$ with an initial uncertainty of $0.8\,\mathrm{m}$ (Petty et al., 2016)."

**Q6:** *Lines 29-31: Since you mention that characterization of sea ice topography is an active area of research (line 28), I would suggest citing more recent studies using laser altimetry and photogrammetry (e.g. Farrell et al. 2020, https://doi.org/10.1029/2020GL090708; Li et al. 2019 https://doi.org/10.3390/rs11070784; and/or others).*

**A6:** Thanks for the references. We have added more recent references as suggested.

- Farrell, S., Duncan, K., Buckley, E., Richter-Menge, J., and Li, R.: Mapping sea ice surface topography in high fidelity with ICESat-2,Geophysical Research Letters, 47, e2020GL090 708, https://doi.org/10.1029/2020GL090708, 2020.
- Li, T., Zhang, B., Cheng, X., Westoby, M. J., Li, Z., Ma, C., Hui, F., Shokr, M., Liu, Y., Chen, Z., Zhai, M., and Li, X.: Resolving Fine-Scale Surface Features on Polar Sea Ice: A First Assessment of UAS Photogrammetry Without Ground Control, Remote Sensing, 11,https://doi.org/10.3390/rs11070784, 2019.
- Nghiem, S., Busche, T., Kraus, T., Bachmann, M., Kurtz, N., Sonntag, J., Woods, J., Ackley, S., Xie, H., Maksym, T., et al.: RemoteSensing of Antarctic Sea Ice with Coordinated Aircraft and Satellite Data Acquisitions, in: Proc. IGARSS., pp. 8531–8534, IEEE, https://doi.org/10.1109/IGARSS.2018.8518550, 2018.

The sentence in Line 29-31 has been updated as:

"The sea ice topography can be measured by various instruments, such as laser altimeters (Dierking, 1995; Schutz et al.,2005; Abdalati et al., 2010; Farrell et al., 2011, 2020) and stereo cameras using photogrammetric techniques (Dotson and Arvesen., 2012, updated 2014; Divine et al., 2016; Nghiem et al., 2018; Li et al., 2019)."

**Q7:** *Line 87: By previous work, do you mean Huang and Hajnsek (2021)? Or previous studies in general?*

**A7:** Sorry for the vague statement. The previous work refers to the work in Huang and Hajnsek (2021). This has been clarified in the revision.

**Q8:** *Line 91: Same as above comment. If previous work is referring to Huang and Hajnsek (2021), I would suggest writing that explicitly.*

**A8:** It has been clarified in the revision.

**Q9:** *Line 179-180: How are water-surface points selected? And how many pixels/points are used in this scene? More information would be useful to ensure that these reference surface elevations are not biased due to e.g. newly frozen leads.*

**A9:** In this study, 9 points/pixels are labeled from DMS images as the water surface. In addition to the information from the optical photo (i.e., DMS images), we also use the information from InSAR coherence magnitude. Since the interferometric coherence measured over water is very low, a coherence map can be used to detect the water in the sea ice cover. All 9 points are verified with InSAR coherence magnitude below 0.3, a threshold of open-water area mask used in (Huang and Hajnsek, 2021). Then, the heights of 9 points are averaged and subtracted from the DMS DEMs to obtain the sea ice topographic height relative to the local sea level.

These explanations have been added in the revision:

"In total, we label nine points as water-surface reference according to the DMS images. Since the interferometric coherence magnitude over water is very low, it can also be used to classify open water (Dierking et al., 2017). All the nine points have an interferometric coherence magnitude below $0.3$, which is the threshold of the open-water area mask in (Huang and Hajnsek, 2021). The average height of the open-water points is subtracted from the DMS DEMs to obtain the sea ice topographic height relative to the local sea level."

**Q10:** *Line 199: How many segments are removed vs used due to mis-coregistration? A percentage of rejected or accepted segments would be useful here.*

**A10:** The percentage of accepted segments is $76\%$, which means $12$ segments are removed due to mis-coregistration, and the rest $38$ segments are accepted for the experiments. The specific numbers have been added in the revision:

"Among the $50$ segments, $12$ segments which still contain residual mis-coregistration induced by the sea ice non-linear movement or rotation are excluded and will not be used in the following experiments. $76\%$ segments from the whole SAR scene are accepted as correctly co-registered segments in this study."

**Q11:** *Figure 8: This figure should have subplots labeled (a-f) on the figure, since they are referenced as such in the text. I agree with reviewer 1 that it is not apparent how phase centers are derived from these figures.*

**A11:** The labels (a-f) have been added in the revision. In the preprint manuscript, Fig. 8 shows the complex coherence, modelled with Eq. (12), in the unit circle. The radius corresponds to the coherence magnitude, the angular rotation to the phase. The phase can be translated to height via

$$h_{\text{volume}} = \frac{\angle\tilde{\gamma}_v}{\kappa_{\text{z\_vol}}} \tag{3}$$

where $\tilde{\gamma}_v$ can be substituted with $\tilde{\gamma}_{\text{mod\_T}}$ derived from Eq. (12) (in the preprint manuscript).

The above equation has been added in Section 2, and the following texts has been added in Section 4.3:

"The sensitivity of $\tilde{\gamma}_{\text{mod\_T}}$ to various parameters is presented in Fig. 9, where the radius and angular rotation corresponds to the coherence magnitude and phase, respectively. The phase can be translated to height via Eq. (3)."

Second, we would like to clarify that the volume-only phase centers are not directly derived from the plots but from Eq. (11) (in the preprint manuscript). The complex value of $\tilde{\gamma}_{\text{v}}(\sigma_1, z_{01})$ can be obtained according to Eq. (11) (in the preprint manuscript), and the phase part is denoted as $\angle\tilde{\gamma}_{\text{v}}(\sigma_1, z_{01})$. The derived phase can be converted to height by Eq. (3). As the range of $\sigma_1$ is $1 - 10\,\text{db/m}$, the corresponding phase center height is calculated to be $-6$ to $-7\,\text{cm}$. Similarly, the phase $\angle\tilde{\gamma}_{\text{v}}(\sigma_2, z_{12})$ can be obtained according to Eq. (11) (in the preprint manuscript) at different values of $\sigma_2$ and converted to height by Eq. (3). Across the range of $\sigma_2$ (i.e., $10 - 200\,\text{db/m}$), the phase center height varies from $-15$ to $-33\,\text{cm}$. These explanations have been added in the revision:

"The complex coherence of the snow volume $\tilde{\gamma}_{\text{v}}(\sigma_1, z_{01})$ can be calculated by Eq. (15) with thickness $z_{01} = 15\,\text{cm}$, and its magnitude and phase can be denoted as $|\tilde{\gamma}_{\text{v}}(\sigma_1, z_{01})|$ and $\angle\tilde{\gamma}_{\text{v}}(\sigma_1, z_{01})$, respectively. Then, the phase center location of the snow volume alone can be calculated by Eq. (3). Across the range of $\sigma_1$ (i.e., $1 - 10\,\text{db/m}$), the snow volume has an individual coherence magnitude (i.e., $|\tilde{\gamma}_{\text{v}}(\sigma_1, z_{01})|$) close to unity and phase center height varying from $-6$ to $-7\,\text{cm}$. Similarly, the ice volume $\tilde{\gamma}_{\text{v}}(\sigma_2, z_{12})$ has an individual coherence magnitude of almost unity and a phase center height between $-15$ to $-33\,\text{cm}$ for the investigated range of ice extinction coefficients."

**Q12:** *Line 393: Similar to above points, what percentage of pixels are processed (i.e. heights above 1.5m) vs not? With a scene-average height of 1.27m along the DMS DEM (line 494), I suspect that a large portion has been removed.*

**A12:** As we explained in A2, in the revision, pixels with height above $0.8\,\text{m}$ have been processed into the model, which take up $83\%$ of the total co-registered pixels. This is added in the revision:

"In order to select the ice that is deformed and thick without seawater flooding, the samples with height above $0.8\,\mathrm{m}$, which are $83\%$ of the co-registered data set, are selected."

**Q13:** *Line 398: I assume 18cm is the average snow depth of the whole region, including ice <1.5m? If only samples >1.5m are selected for processing (line 394) I am curious how your results would look if you were able to use snow depth on just the ice with elevation >1.5m. While I know this information may not be available, using some type of spatially varying snow depth assumption may help to constrain possible retrieved topographies.*

**A13:** Yes, $18\,\mathrm{cm}$ is the average snow depth of the whole region due to the limited spatial resolution of available snow measurements. The reply to this comment is a repetition from an earlier answer (**A4**). In the revision, we have performed the whole inversion scheme and retrieved heights with various snow depths from $-0.05\,\mathrm{m}$ to $-0.75\,\mathrm{m}$. We also have emphasized that this type of varying snow depth assumption will help to constrain possible retrieved topographies, see **A4** for details.

**Q14:** *Figure 13: It's fairly tough to see the DMS DEM in between grey lines in (b)-(d) and draw any conclusion about its agreement with the SAR data. I would recommend making the lines thinner or reducing the width of the zoomed sections, if possible, so that more of the DMS heights are shown. If inclined, a difference map (InSAR height – DMS height) would be useful to provide a more quantitative 2-D verification.*

**A14:** The width of the zoomed sections has been reduced, and Figure 13 has been updated in the revision, see Fig. 5(b)-(d) in this document. Besides, the relative retrieval bias $\epsilon = (h_{\mathrm{mod\_S}} - h_{\mathrm{DMS}})/h_{\mathrm{DMS}}$ of zoom-in area 1-3 have been included in the revision to provide a more quantitative 2-D verification, see texts and Fig. 5 (e)-(g):

"The relative retrieval bias $\epsilon$, which can be calculated as $\epsilon = (h_{\mathrm{mod\_S}} - h_{\mathrm{DMS}})/h_{\mathrm{DMS}}$, is used to quantify the retrieval accuracy. In Fig. 5(e)-(g), $\epsilon$ over Area 1-3 are below $25\%$ for most parts, whereas only a few parts, often near to the masked-out regions (pixels in transparent), present higher $\epsilon$. Note that the masked-out regions refer to water and thinner ice areas with height less than $0.8\,\mathrm{m}$. The averaged $\epsilon$ over Area 1-3 are about $19\%$, $14\%$, and $15\%$, respectively, and is $18\%$ for the whole image, achieving the theoretical $25\%$-error accuracy derived in Section 4.4."

**Q15:** *Figure 13 also: How are heights less than 1.5m calculated in this SAR image if not selected for processing with this model? Subplot (d) in particular appears to have regions of 0m height that I suspect are not entirely physical.*

**A15:** In the revision, the height threshold has been changed to be $0.8\,\mathrm{m}$, and the height below $0.8\,\mathrm{m}$ have been masked out. Therefore, in the updated retrieval map (see Fig. 5 in this document), the retrieved height and DMS measurements below $0.8\,\mathrm{m}$ have been set to be transparent and would not be considered in the analyses.

**Q16:** *Line 456: I would suggest clarifying that $h_{Model}$ in this case is the simplified model. While I understand it is in the "simplified model" section, to me the third row in Table 1 is the Theoretical model row (as it is the third method). The fact that the RMSE ranges between 0.22 and 0.27 for both models further adds to the confusion.*

**A16:** Sorry for the confusion. The statements have been modified as suggested in the revision:

"Table 1 summarizes the performances between the retrieved height from the simplified model and $h_{\mathrm{DMS}}$ for the four polarizations."

**Q17:** *Line 487: This line (particularly "larger baselines respectively larger kz values") doesn't quite sound correct as written. Do you perhaps mean the possessive "baselines"?*

**A17:** The larger baseline means a larger value of the effective perpendicular baseline $b_{\perp}$ (Eq.4 in the preprint manuscript)

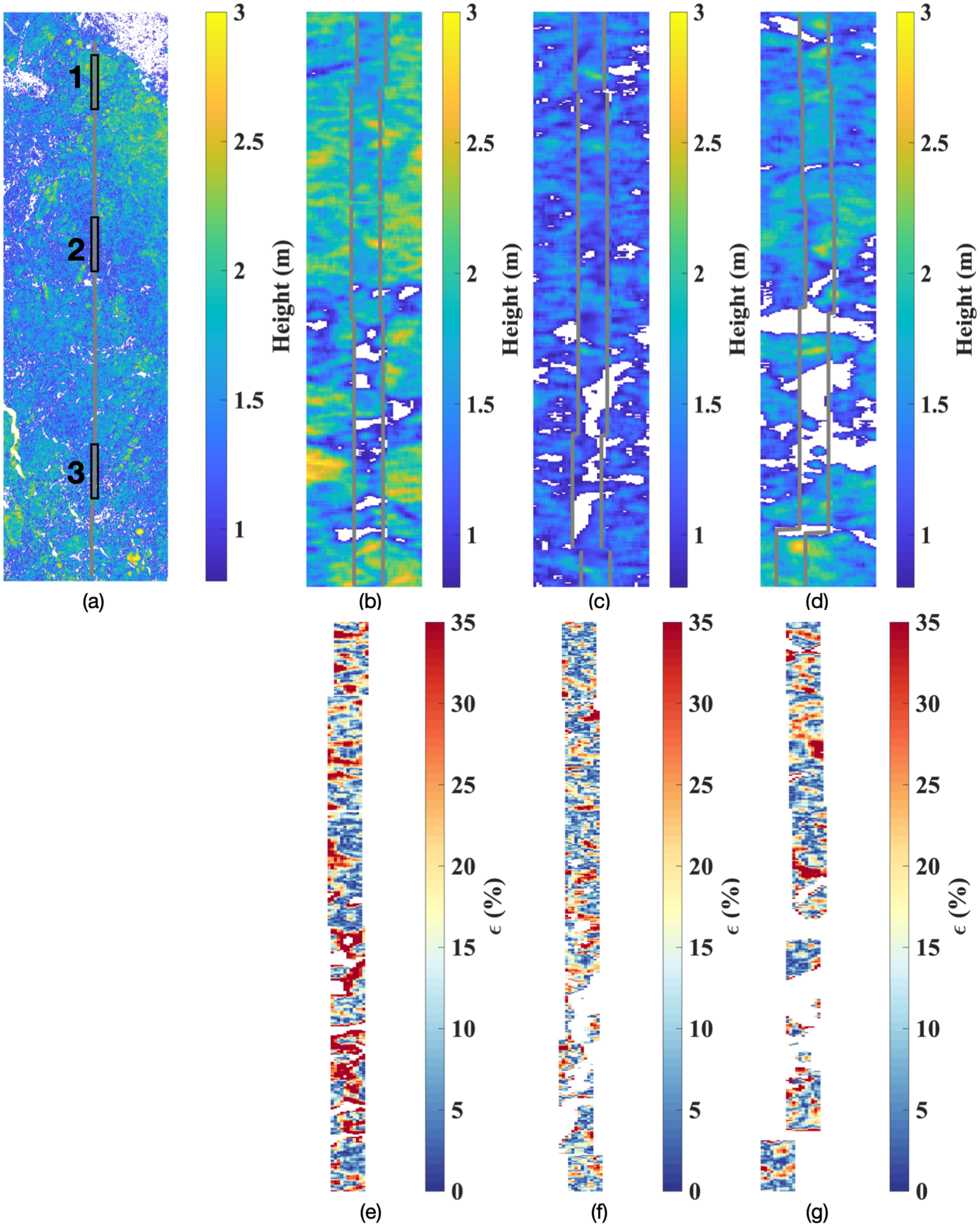

Fig. 5: Sea ice topographic retrieval with the simplified model ($h_{\text{mod\_S}}$). The transect from the DMS DEM is plotted between grey lines. Note that the heights below $0.8\,\text{m}$ are set to be transparent. (a) The whole studied SAR image. (b)-(d) Zoom-in of Areas 1-3. (e)-(g) Relative retrieval bias $\epsilon = (h_{\text{mod\_S}} - h_{\text{DMS}})/h_{\text{DMS}}$ of Area 1-3.

in the interferometric SAR configuration. It has been clarified in the revision:

"It reveals the potential to establish an inversion scheme by combining observations from a range of different $\kappa_z$ (i.e., the vertical wavenumber in free space), where larger values of the effective perpendicular baseline $b_\perp$, corresponding to larger $\kappa_z$ values, are expected to improve height retrieval accuracy."

**Q18:** *Line 499: Should be "25%-error accuracy" to be consistent with previous sections*

**A18:** It has been corrected to be "25%-error accuracy".

**Q19:** *Technical Corrections:*

- *Line 59: Icebridge -> IceBridge*
- *Line 143: iceberg -> icebergs*
- *Figure 1 caption: rectangular -> rectangle*
- *Line 215: 'flat-earth removed' should be written as 'flat-earth-removed'*
- *Line 254: Provide full names of TDF and TSX at first mention*
- *Line 470: (grammar) well correct -> e.g. adequately/sufficiently/suitably correct*
- *Line 501: comma after "For instance"*

**A19:** All above points haven been corrected in the revision.

Again, we sincerely thank the editor and reviewers for helping us improving the manuscript.